Unclassified
SECURITY CLASSIFICATION OF THIS PAGE

(2)

AD-A216 739 DOCUMENTATION PAGE

Form Approved
OMB No. 0704-0188

1a. REPORT SECURITY CLASSIFICATION: Unclassified	1b. RESTRICTIVE MARKINGS
2a. SECURITY CLASSIFICATION AUTHORITY	3. DISTRIBUTION/AVAILABILITY OF REPORT: Approved for public release; distribution is unlimited.
2b. DECLASSIFICATION/DOWNGRADING SCHEDULE	
4. PERFORMING ORGANIZATION REPORT NUMBER(S)	5. MONITORING ORGANIZATION REPORT NUMBER(S): AFOSR-TR- 89-1879
6a. NAME OF PERFORMING ORGANIZATION: Stanford University; 6b. OFFICE SYMBOL (If applicable)	7a. NAME OF MONITORING ORGANIZATION: AFOSR/NA
6c. ADDRESS (City, State, and ZIP Code): Department of Mechanical Engineering, Stanford University, Stanford, CA 94305	7b. ADDRESS (City, State, and ZIP Code): Building 410, Bolling AFB DC 20332-6448
8a. NAME OF FUNDING/SPONSORING ORGANIZATION: AFOSR/NA; 8b. OFFICE SYMBOL (If applicable): NA	9. PROCUREMENT INSTRUMENT IDENTIFICATION NUMBER: AFOSR 84-0373
8c. ADDRESS (City, State, and ZIP Code): Building 410, Bolling AFB DC 20332-6448	10. SOURCE OF FUNDING NUMBERS: PROGRAM ELEMENT NO. 61102F; PROJECT NO. 2308; TASK NO. A2; WORK UNIT ACCESSION NO.

11. TITLE (Include Security Classification)
(U) An Investigation of Flow Structure, Mixing and Chemical Reaction in Combusting Turbulent Flows

12. PERSONAL AUTHOR(S)
Brian J. Cantwell and Craig T. Bowman

13a. TYPE OF REPORT	13b. TIME COVERED	14. DATE OF REPORT (Year, Month, Day)	15. PAGE COUNT
Final Technical Report	FROM 9/1/84 TO 6/30/89	October 23, 1989	31 pages

16. SUPPLEMENTARY NOTATION

17. COSATI CODES			18. SUBJECT TERMS (Continue on reverse if necessary and identify by block number)
FIELD	GROUP	SUB-GROUP	Combustion, Reacting Flows, Turbulent Mixing, Diagnostics, Particle Tracking, Flow Topology
21	01		
21	02		

19. ABSTRACT (Continue on reverse if necessary and identify by block number)

An experimental investigation of the relationship between flow structure and flame structure in a low-speed, co-flowing, non-premixed, methane-air jet diffusion flame has been completed. The purpose of the research was to examine the spatial structure of the unsteady reaction process as it relates to the unsteady velocity field and to use topological methods in the interpretation of flame dynamics. A small, acoustically produced, perturbation in the fuel jet velocity was used to phaselock the basic flickering instability of the flame thus creating a very periodic and controllable flow, suitable for conditional sampling. Various diagnostic techniques were used in the research including single-component laser anemometry, direct and schlieren photography, Mie scattering from seed particles introduced into the flow, planar, laser-induced fluorescence the OH radical and particle tracking for measuring instantaneous planar velocity field data. Velocity fields have been measured as a function of the phase of the flickering cycle over the first 20 diameters of the flame. Radiation from soot appears in the particle track images and

20. DISTRIBUTION/AVAILABILITY OF ABSTRACT: ☒ UNCLASSIFIED/UNLIMITED ☒ SAME AS RPT. ☐ DTIC USERS	21. ABSTRACT SECURITY CLASSIFICATION: Unclassified
22a. NAME OF RESPONSIBLE INDIVIDUAL: Julian M Tishkoff	22b. TELEPHONE (Include Area Code): (202) 767-4964 / 4936 — 22c. OFFICE SYMBOL: AFOSR/NA

DD Form 1473, JUN 86 — Previous editions are obsolete. — SECURITY CLASSIFICATION OF THIS PAGE

Unclassified

serves as a useful reference for the flame location and shape. Some of this data has been overlaid on the OH data to reveal the flame-flow interaction. In an effort to better understand the fluid mechanics of the flame an investigation has also been carried out of a co-flowing helium jet. This flow has the same overall density variation and exhibits a vortex shedding instability reminiscent of the flickering of the flame. The particle tracking technique has been used to measure unsteady velocity fields in the helium jet and topological methods have been used to make comparisons between the two flows. The main results of the research are as follows:

1) The effect of increasing pressure is to cause a moderate decrease in the visual flame height and to produce small-scale motions through decreased relative diffusion.

2) The OH images show that the flame zone is located outside of and approximately parallel to the luminous soot region.

3) When the flame is forced at a frequency close to the natural flickering frequency, the flame pinches off and the flow breaks up into a series of distinct eddies with a fine structure which is highly repeatable from cycle to cycle. This repeatability of the fine scales is also observed in the helium jet for Richardson numbers greater than one. The phenomenon is only observed in the presence of co-flow which eliminates the random meandering typical of buoyant plumes in a quiescent environment.

4) Velocity measurements taken near the jet exit in the flame and helium jet reveal a significantly different initial flow development. In the diffusion flame the instability of the cylindrical plume rising from the point of ignition and the buoyant acceleration of fluid on the jet axis play a dominant role in triggering the flickering instability at a point several diameters downstream of the jet exit.. Whereas in the helium jet buoyancy is released in a distributed manner across the jet exit and flow acceleration on the axis begins immediately. The contrasting manner in which buoyancy is released is thought to account for significant differences in frequency scaling and controllability between the two flows.

5) The flickering instability and flame pinch-off is observed to involve a distinct birth, growth and decay cycle of a cellular vortex-ring-like buoyant thermal which rises with a nearly constant velocity and is located below the visible flame. Topological methods are found to be useful for characterizing this flow structure which consists of three critical points; a saddle point near the base of the flame, a saddle point near the flame tip and a center which surrounds the base of the flame. The saddle point near the base of the flame is associated with flame extinction observed in the OH images.

6) Typical levels of flow divergence are found to be comparable to typical levels of vorticity in the flame suggesting that volumetric expansion associated with heat release should be included in models of flame-vortex interaction.

7) The instantaneous rate of strain field deduced from the velocity measurements indicates that the principal direction of compressive strain has a strong tendency to be aligned normal to the flame front except in regions where the flame is undergoing rapid rotation.

8) The time evolution of the flame has been studied by following the paths of the critical points in the three-dimensional space of invariants of the local deformation tensor. An examination of this path clearly reveals the birth, growth and decay cycle referred to earlier. Flame pinch-off is a very well defined event with all of the invariants of the critical points tending rapidly to zero after the event.

This project constitutes the first detailed study of unsteady flame topology. The results suggest that complex reacting flow fields can be described in terms of a limited set of elementary flow patterns and that the invariants of the deformation tensor can serve as a sensitive indicator of flame dynamics. This is a new and potentially fruitful line of inquiry which may have significant applications to the interpretation of complex three-dimensional flow fields and to a broad range of fundamental problems in turbulent combustion.

Department of AERONAUTICS and ASTRONAUTICS
STANFORD UNIVERSITY

AN INVESTIGATION OF FLOW STRUCTURE, MIXING AND CHEMICAL REACTION IN COMBUSTING TURBULENT FLOWS

Final Technical Report

AFOSR Grant Number 84-0373

September 1, 1984 to June 30, 1989

Brian J. Cantwell

Department of Aeronautics and Astronautics
Stanford University
Stanford, California 94305

SUMMARY

An experimental investigation of the relationship between flow structure and flame structure in a low-speed, co-flowing, non-premixed, methane-air jet diffusion flame has been completed. The purpose of the research was to examine the spatial structure of the unsteady reaction process as it relates to the unsteady velocity field and to use topological methods in the interpretation of flame dynamics. A small, acoustically produced, perturbation in the fuel jet velocity was used to phaselock the basic flickering instability of the flame thus creating a very periodic and controllable flow, suitable for conditional sampling. Various diagnostic techniques were used in the research. Early on, measurements of the unsteady velocity field at several different ambient pressures were obtained using single-component laser anemometry. In addition, flow visualization experiments were conducted using direct and schlieren photography and Mie scattering from seed particles introduced into the flow. Planar, laser-induced fluorescence images of the OH radical, which provide information on the instantaneous location of the reaction zone, were also obtained. More recently, a particle tracking technique was developed to facilitate acquisition of instantaneous planar velocity field data. Velocity fields have been measured as a function of the phase of the flickering cycle over the first 20 diameters of the flame. Radiation from soot appears in the particle track images and serves as a useful reference for the flame location and shape. Some of this data has been overlaid on the OH data to reveal the flame-flow interaction. In an effort to better understand the fluid mechanics of the flame an investigation has also been carried out of a co-flowing helium jet. This flow has the same overall density variation and exhibits a vortex shedding instability reminiscent of the flickering of the flame. The particle tracking technique has been used to measure unsteady velocity fields in the helium jet and topological methods have been used to make comparisons between the two flows. The main results of the research are as follows:

1) The effect of increasing pressure (or Reynolds number) is to cause a moderate decrease in the visual flame height and to produce small-scale motions through decreased relative diffusion. The large-scale structure and response to excitation remains more or less unchanged.

2) The OH images show that the flame zone is located outside of and approximately parallel to the luminous soot region. The OH images also provide an approximate measure of reaction zone thickness which is 2mm for the conditions studied (1 atm.).

3) When the flame is forced at a frequency close to the natural flickering frequency, the flame pinches off and the flow breaks up into a series of distinct eddies with a fine structure which is highly repeatable from cycle to cycle. This repeatability of the fine scales is also observed in the helium jet for Richardson numbers greater than one. The phenomenon is only observed in the presence of co-flow which eliminates the random meandering typical of buoyant plumes in a quiescent environment.

4) Detailed velocity measurements have been taken near the jet exit in the flame and helium jet and reveal a significantly different initial flow development. In the diffusion flame the instability of the cylindrical plume rising from the point of ignition and the

buoyant acceleration of fluid on the jet axis play a dominant role in triggering the flickering instability at a point several diameters downstream of the jet exit.. Whereas in the helium jet buoyancy is released in a distributed manner across the jet exit and flow acceleration on the axis begins immediately. The contrasting manner in which buoyancy is released is thought to account for significant differences in frequency scaling and controllability between the two flows.

5) The flickering instability and flame pinch-off is observed to involve a distinct birth, growth and decay cycle of a cellular vortex-ring-like buoyant thermal which rises with a nearly constant velocity and is located below the visible flame. Topological methods are found to be useful for characterizing this flow structure which consists of three critical points; a saddle point near the base of the flame, a saddle point near the flame tip and a center which surrounds the base of the flame. The saddle point near the base of the flame is associated with flame extinction observed in the OH images.

6) Typical levels of flow divergence are found to be comparable to typical levels of vorticity in the flame suggesting that volumetric expansion associated with heat release should be included in models of flame-vortex interaction.

7) The data has been used to determine the instantaneous rate of strain field. The results indicate that the principal direction of compressive strain has a strong tendency to be aligned normal to the flame front except in regions where the flame is undergoing rapid rotation.

8) The time evolution of the flame has been studied by following the paths of the critical points in the three-dimensional space of invariants of the local deformation tensor. An examination of this path clearly reveals the birth, growth and decay cycle referred to earlier. Flame pinch-off is a very well defined event with all of the invariants of the critical points tending rapidly to zero after the event.

This project constitutes the first detailed study of unsteady flame topology. The results suggest that complex reacting flow fields can be described in terms of a limited set of elementary flow patterns and that the invariants of the deformation tensor can serve as a sensitive indicator of flame dynamics. This is a new and potentially fruitful line of inquiry which may have significant applications to the interpretation of complex three-dimensional flow fields and to a broad range of fundamental problems in turbulent combustion.

BACKGROUND AND RESEARCH OBJECTIVES

Recent research in turbulent combustion has focused on establishing appropriate models for the interaction between turbulence structure and flame chemistry. Although our understanding of the physics of mixing and combustion has improved, there is a need for data which directly reveal the coupling between the unsteady velocity field and the unsteady reaction field in a combusting flow. The objective of the present work is to combine time-resolved field measurements of velocity and flame structure in a time-dependent hydrocarbon-air flame. Interpretation of the results employs topological methods which have been used to characterize the structure of non-reacting flows. This methodology provides a unified approach for characterizing various strain and rotation fields which can occur in turbulent flows. The work has lead to an improved understanding of the sequence of flow events leading to the breakup of unsteady diffusion flames and to a better understanding of the relationship between flame structure and the instantaneous strain rate field. Information of this type will contribute to improved models and numerical simulations of combustion.

STATUS OF THE RESEARCH

The configuration investigated in this study is a co-flowing, non-premixed jet flame, with methane in the core flow and air in the surrounding flow. The methane passes through a small chamber containing a loudspeaker which can be used to add a velocity perturbation to the core flow at various frequencies and amplitudes. Results obtained during the first three years of the program are reported in publications 1 through 7. During the final year and a half of the program, the following tasks were completed.

1) Final Development and Application of a Particle Tracking Technique for Making Planar Velocity Field Measurements

Figure 1 shows a typical processed image of the vector field data measured using this technique. In the original photograph each track is identifiable as a sequence of three dots forming a straight line. The photographs, which also contain the soot radiation image, are digitized using a DEST scanner interfaced to a MacII with a maximum resolution of 300 dots per inch. In the final year of the grant, software development for the MacII has been completed which converts the image data to velocity vector field information. The algorithm is based on a search technique which first locates the centroids and diameters of all the particles in the field. Once these have been identified an initial particle is chosen and the program proceeds outward on a series of circles of increasing radius until a nearest neighbor is identified. This defines a conical region within which a further search is carried out to identify a third particle which is collinear with the first two. If the second search is successful a velocity vector is formed. All the particles in the image are processed in this fashion with due consideration to particle overlap and possible repeat encounters with the same particle. Processing of a typical image takes approximately one to two minutes depending on the number of particles which have to be processed. Both the inner and outer flow fields have been seeded with Aluminum oxide particles. Images of the velocity vector field and soot radiation obtained at various phases of the excitation cycle allow observation of the unsteady development of the flame.

2) Measurements of Planar Velocity Vector Fields in the Flame

Complete vector fields were measured by Lewis (1989) over the first 20 diameters above the fuel jet exit. Processed images of the complete data set are shown in Figures 2 a-d. Each of these images is constructed from a series of 3cm high slices taken at different times and discontinuities in the soot boundary can be seen where adjacent images meet. The fact that the images match up as well as they do is evidence of the high cycle-to-cycle and day-to-day repeatability of the flow. Initially our interest was focused primarily on the region from 14 to 25 cm where flame pinch-off occurs. Although images were made of the jet exit region it was only very recently, a considerable time after the downstream images were processed and the flame apparatus was no longer available, that we fully appreciated the need to see what was going on upstream. Fortunately the image data from this region was available however because we did not initially anticipate how it might eventually be used there is a gap in the data between 12 and 14 cm above the jet exit.

3) Interpolation of Vector Field Data

Particle tracks appear at random locations in the photographs and considerable effort was expended in the last year and a half to develop a method of interpolation onto a uniform grid. Figures 3 a and b show typical examples of the raw and interpolated data at four streamwise locations indicated by horizontal lines through the accompanying vector field image. The open circles in these figures are the raw data for the axial and radial velocity components respectively and the solid lines are the interpolation function. The spacing and density of raw data in these figures are indicative of some of the limitations of the particle tracking method. For reasons discussed by Lewis (1989) the flame itself tends to contain relatively few particle tracks leading to gaps in the spanwise profiles which the interpolation method must cope with. Overlapping data, particularly in the radial component, tends to exhibit quite a bit of scatter. Therefore a simple scheme designed to pass through all of the data could not be used. On the other hand it was necessary for the technique to reproduce the raw data as well as possible where it existed. The details of how this was accomplished along with estimates of the uncertainty in the raw and interpolated data are given in Lewis (1989). We have used the interpolated data to generate vorticity and strain rate information. Generally speaking the results are quite satisfactory and of a quality comparable to or better than any other available technique.

4) Study of the Flame Strain Rate Field

Figure 4 a-d depicts the compressive strain field derived from the interpolated velocity data. The strain rate tensor is symmetric and therefore has real eigenvalues with orthogonal eigenvectors. The lines plotted in Figures 4 a-d are aligned with and proportional to the compressive eigenvector of the strain tensor. The most interesting feature of these figures is that the compressive strain rate direction has a strong tendency to be aligned normal to the flame front (taken to be the outside boundary of the soot envelope) particularly after the flame has pinched off as can be seen most clearly in the upper portion of Figures 4 a and d. The largest deviation from this tendency occurs in regions where the vorticity is high, particularly where the flame is being rolled up but

also in the early region of the flame where there are high levels of vorticity along the flame front. In these regions the direction of compressive strain can be at a very oblique angle and in some areas almost parallel to the flame front. Local models of strained flames usually assume that the flame sheet is normal to the compressive component of the strain rate and tend to ignore the role of vorticity which can be responsible for large deformation rates along the flame front.

5) Study of Flame topology

The velocity measurements were used to picture the topology of a flame undergoing breakup. There exists in this flow a relatively unambiguous means of choosing the most appropriate frame of reference from which to view the velocity vector field. As the flickering instability develops a confined region of high strain rate develops on the axis several jet diameters downstream of the fuel jet exit. Figure 4 shows the axial velocity measured along the centerline of the flame. The first evidence of the high-strain-rate disturbance can be seen in Figure 4 phase 7 at an axial position of about 3-5 cm. Although there are significant buoyancy-induced accelerations inside the flame the high strain rate disturbance moves vertically upward (see Figure 4, phases 7, 8, 1, 2, etc.) at a nearly constant speed and the velocity fields in Figures 1 - 4 are plotted with respect to an observer moving at this speed.

Figure 1 indicates various salient features of the flame including the image produced by soot radiation which appears as a heavy black envelope surrounding the fuel-rich core of the flame. Several critical points are indicated; a lower saddle, which in this figure is indicated at the top near the flame tip, an outer ring vortex beneath the flame surrounding the flame neck and an upper saddle located at the base of the flame.

It should be emphasized that the topology of the velocity vector field does depend on the frame of reference. In Lewis, Cantwell, Vandsburger and Bowman (1988) the topology was discussed with respect to an observer moving with the lower boundary of the flame which tends to move somewhat more slowly than the region of high strain rate. In this frame of reference the on-axis saddle near the flame tip splits into an off - axis saddle which surrounds the flame tip. After considering various possible choices for the moving frame we have concluded that a reference frame moving with the region of high strain rate is the best choice in that it produces the simplest topology and the most slowly varying flow field and seems to provide the best insight into the various events leading up to flame breakup.

The reason for the apparent ambiguity in naming the saddles has to do with the periodicity of the flame and the fact that they are really part of the same flow structure which tends to be located between adjacent rolled-up flames. This is made clear in Figure 6 which depicts a sequence of frames showing the complete evolution of flame topology during the flickering cycle over the first 20 diameters of the flow. The dashed line in this figure corresponds to the soot envelope seen in Figure 1. The necking down and eventual pinching off of this envelope leads to the breakup of the flame. This figure indicates that the flickering instability in a diffusion flame involves a distinct birth, growth and decay

cycle of an expanding, cellular, vortex-ring-like, buoyant thermal. This buoyant thermal originates at a point 3-5 diameters downstream of the jet exit and is associated with the high strain rate disturbance described earlier. As the thermal develops, the soot envelope is distorted into a tent-like shape with the flow near the upper saddle tending to stretch the envelope outward, rolling it up into the center, while the movement of air toward the axis near the lower saddle tends to push the envelope inward eventually causing the flame to pinch off. The relatively rapid growth of the thermal and concomitant increase in its apparant mass act to offset the acceleration by buoyancy helping to explain the observed constant speed of this flow structure.

The flicker instability is driven by, but not soley dependent upon, buoyancy and some understanding of the basic mechanism can be gained by examining velocity data very near the jet exit. The release of heat in a cylindrical sheet surrounding the jet exit creates a hollow, cylindrical plume which rises under the action of buoyancy. The acceleration of fluid on the jet axis begins slowly but becomes stronger as heat is conducted to the jet centerline. As the flow accelerates the flame sheet contracts, further increasing the rate of heat transfer to the centerline, further accelerating the flow, further increasing the heat transfer and so forth. Also contributing to the acceleration and pinch-off on the centerline is the diffusion of momentum radially inward due to the opposite signed vorticity contained in the flame generated plume. This opposite signed vorticity is produced within a couple of diameters of the jet exit and persists for a considerable distance downstream. As the flame sheet pinches off this vorticity accumulates near the upper saddle giving it a peculiar re-entrant appearance imparting a heart shape to the overall structure as sketched in Figure 6. The thermal vortex structure retains this heart-shape until the vorticity at the upper saddle is convected outward and downward into the center terminating the flickering cycle.

Figure 7 depicts the evolution of the flow in P, Q, R coordinates corresponding to the three invariants of the deformation tensor evaluated at the critical point. The velocity derivatives have been normalized by the jet exit velocity and jet diameter. To simplify the discussion each invariant is plotted on a separate set of axes. The first invariant, P, is the negative of the flow divergence and is related to heating and cooling of fluid in the neighborhood of the critical point. A feeling for the relative magnitude of P can be gained by examining Figure 7 (d) which indicates the magnitude of the strain and vorticity at the critical points. The normalized vorticity at the center attains a maximum value of 5 compared to normalized values of P at the saddles which lie between -2 and 2. In other words typical levels of flow divergence are comparable to typical levels of vorticity and can be expected to play a significant role in the flow dynamics. The flow divergence at the center remains very close to zero over most of the cycle. The birth of the vortex structure occurs at Phase 2 with the first appearance of critical points in this frame of reference. The value of P at the lower saddle tends to remain negative indicating a slowly decreasing density probably related to heating at the saddle through conduction. The upper saddle seems to begin with relatively rapid cooling possibly associated with the convection along the axis of relatively cooler core fluid as the soot envelope is pushed outward.

The second invariant, Q, corresponding to the sum of cofactors is shown in Figure 7 (b). The centers (really a line surrounding the jet axis) show a slowly increasing value of Q, indicating more intense rotation, until flame pinch-off occurs after which Q falls almost to zero. An examination of the time evolution of Q and R the determinant of the deformation tensor (Figure 7 c) clearly reveals the birth, growth and decay cycle referred to earlier. Flame pinch-off is a very well defined event with all of the invariants of the critical points tending rapidly to zero after the event. Another feature which is revealed is that the upper and lower saddle points have a very different character. Figure 7 (d) indicates that the magnitude of the axial extensive strain at the lower saddle is considerably smaller than the magnitude of the axial compressive strain at the upper saddle. This difference becomes even more apparent when R, which is proportional to the cube of the strain rates, is plotted in Figure 7 (c). This figure depicts a rapid build-up and then fall-off of R at the upper saddle while R at the center and lower saddle remains close to zero throughout the cycle. Although we have just begun to study the topology of flames in (P, Q, R) space these initial results suggest that the invariants of the deformation tensor can serve as a sensitive indicator of flame dynamics.

6) Planar Measurements of the Velocity Vector Field in the First 5 Diameters of the Helium Jet.

Strawa and Cantwell (1989) studied the flame at several ambient pressures. Increasing the pressure has the effect of increasing the Reynolds number without decreasing the Richardson number. This approach permits one to study a low-speed, high Reynolds number flame with co-flow. Similar conditions can be produced at atmospheric pressure only by increasing the scale of the apparatus as, for example, in the study of pool fires but this complicates the introduction of co-flow. It was found in this study that when the forcing was at a frequency close to the natural flickering frequency of the flame that the flame broke up into a series of distinct eddies with fine scale motions which were highly repeatable from cycle to cycle. In order to study this phenomenon Subbarao (1987) carried out an extensive, systematic study of the effect of Reynolds number and Richardson number on the structure of a helium-air co-flowing jet. The Helium to Air density ratio is about 7 which is comparable to the nominal hot products to cold air density ratio in the flame. It was therefore felt that the helium jet might provide a good model of the hydrodynamic behavior of the flame and might help us isolate the effects of buoyancy from the effects of heat release. It was found that at a Richardson number of 1.6, a jet Reynolds number (based on the Helium kinematic viscosity) of 390 and 790 and a jet exit to co-flow velocity ratio of 2 that the helium jet also exhibited an extremely repeatable fine scale structure in a manner similar to the flame.

The particle tracking technique was used by Lewis (1989) to study the helium jet under these conditions for the Re = 390 case. High speed movies of the helium jet suggested that the transition to turbulence and repeatability of fine scales were related to the vortex formation process occuring very near the jet exit. Velocity vector fields were measured over the first five diameters of the jet and the interpolated fields are shown in Figures 8 a ,b. The birth - growth - and - decay cycle, which originates at about 3-5 diameters in the flame, begins right at the jet exit in the helium jet. Similarly, whereas

significant flow acceleration on the axis of the flame begins at about 3-5 diameters, flow acceleration begins right at the exit in the helium jet as can be seen in the axial velocity profiles in Figure 9. In general the formation of vortex structures occurs much more quickly in the helium jet.

7) Study of the Flow Field Near the Jet Exit in the Flame and Helium Jet

Our studies suggest that one might understand the frequency scaling and controllability of flickering flames by distinguishing various cases on the basis of how buoyancy is released near the jet exit. At one limit is the diffusion flame where the buoyancy is released in a relatively thin cylindrical sheet. The complex interplay between the jet exit velocity field, the position of the flame sheet and the stability of the plume which rises from the point of ignition makes the downstream development of the flame extremely sensitive to perturbations of the jet exit flow and complicates the diameter dependence of the flickering frequency (Strawa and Cantwell 1989). At the other limit is the helium jet where the buoyancy is released more-or-less uniformly across the entire jet cross-section. The complicating effects of chemical reactions and the associated local instabilities of the flame sheet are removed while retaining approximately the same density ratio of hot combustion products to air. The natural frequency of the helium jet was shown by Subbarao (1988) to scale accurately on the buoyancy time scale. The vector fields measured by Lewis (1989) include extensive data very near the jet exit for both flows. Axial velocity profiles at 1, 2 and 3 diameters as a function of phase are shown in Figures 10 and 11 for the flame and helium jet respectively. The unsteady development of a double peaked velocity profile associated with the flame induced plume is clearly discernible in Figure 10. Whereas the helium data retains a single peak throughout the flickering cycle as can be seen in Figure 11. Recently Mahalingam (1989) has studied the stability of a velocity profile derived from the mean exit flow data of Lewis (1989). An unstable coupled mode associated with the double peak was found with a frequency of 12 Hz and a wavelength of 6.8 cm compared to 16 Hz and 9.5 cm measured by Lewis. The mode shape was similar to the shape of the measured velocity fluctuation profile.

A flow is convectively unstable if a small transient is convected away from where it is generated, ultimately leaving the flow at that location undisturbed, and absolutely unstable if a small disturbance grows exponentially at the location of its generation. Generally speaking convectively unstable flows are easier to control and are sensitive to external forcing. On the other hand absolutely unstable flows tend to be insensitive to external forcing. At zero Richardson number, the stability of the co-flowing jet is determined by the stability of the initial shear layer which is convectively unstable. As the Richardson number is increased the jet becomes absolutely unstable and the flow described in this report would be considered absolutely unstable; the insensitivity of the helium jet to forcing at the jet exit is consistent with absolutely instability.

Visually, the schlieren image of the helium jet is very similar to that of a low speed diffusion flame (cf. Figure 7 in Strawa and Cantwell 1989). Under certain conditions of forcing, at moderate Reynolds numbers, the fine scale structure of the flame is highly repeatable (cf. Figure 7a in Strawa and Cantwell 1989). In fact the unexpected

repeatability observed in the flame was one of the primary motivations of the helium study which began as an attempt to set up a simple experimental model of flame hydrodynamics. There are however fundamental differences between the two flows and these are seen most clearly in their contrasting response to forcing. Whereas the structure of the helium jet can not be easily modified, the diffusion flame can be altered drastically through small perturbations of the jet exit velocity. The high degree of sensitivity of the flame appears to be related to the manner in which buoyancy is released at the jet exit in the form of a cylindrical plume with its own inherent stability properties. Several researchers have reported that jet diffusion flames display a flickering instability whose frequency lies between 9 and 15 Hz for a wide variety of fuels, flow velocities and jet diameters. Whereas the charactertistic frequency of large scale vortex formation in pool fires, for example, is observed to follow a buoyancy time scale. The helium jet exhibits a natural frequency between 15 and 50Hz which, for Richardson numbers above one scales accurately on the buoyancy time scale of the exit flow adding further evidence that the frequencies of natural oscillations in flames depend critically on precisely how the combustion process is distributed near the origin of the flame. The issue of convective versus absolute instability in diffusion flames is complicated by these considerations. An unstable flame will continue to flicker even after perturbations are removed yet its structure is easily modified by the addition of perturbations. This suggests that this catagorization is probably too limited to be useful in the description of flame stability.

CONCLUSIONS

This research was motivated by a desire to examine the spatial structure of the unsteady reaction process as it relates to the unsteady velocity field in a diffusion flame and to use topological methods in the interpretation of flame dynamics. The case chosen for study is representative of a broad class of low speed flames which arise in practical applications. Comparisons of the controllability and natural frequency dependence of both the helium jet and the flame lead to the conclusion that the downstream development of this class of flows is strongly dependent on the detailed mechanism by which buoyancy is released near the origin of the flow.

The time evolution of the flame has been studied by viewing the flow in a frame of reference moving with a high strain rate disturbance which originates 3-5 diameters downstream of the jet exit. The flickering instability and flame pinch-off is observed to involve a distinct birth, growth and decay cycle of a cellular vortex-ring-like buoyant thermal which rises with a nearly constant velocity and is located below the visible flame. Topological methods are found to be useful for characterizing this flow structure which consists of three critical points; a saddle point near the base of the flame, a saddle point near the flame tip and a center which surrounds the base of the flame The saddle point near the base of the flame is associated with flame extinction observed in images of the OH radical.

The interpretation of unsteady flame behavior is carried out by following the paths of the critical points in the three-dimensional space of invariants of the local deformation

tensor. An examination of this path clearly reveals the birth, growth and decay cycle mentioned above. Flame pinch-off is a very well defined event with all of the invariants of the critical points tending rapidly to zero after the event. Although we have just begun to study the topology of flames in (P, Q, R) space these initial results suggest that the invariants of the deformation tensor can serve as a sensitive indicator of flame dynamics.

It is clear from the results of the flame study and the study of a helium jet that buoyancy in the presence of co-flow can lead to an extremely regular and repeatable flow structure over a wide range of scales at Reynolds numbers where the jet would ordinarily be considered turbulent. In the treatment of buoyancy generated turbulence in flames, plumes and thermals the usual picture of the cascade of turbulent kinetic energy from large to small scales, and the local isotropy of the small scales is applied with little change except to incorporate the extra terms in the transport equations which arise in the presence of gravity. The underlying assumption is that scale separation is equivalent to scale independence and that the fine scales can be treated as random. The results of this study stand in contrast to this picture. They depict a flow at moderate Reynolds number where the fine scale motions are not random, but are organized and repeatable from cycle to cycle, and suggest that some rethinking is necessary in the modeling of small scale dissipative motions in buoyant turbulent reacting flows.

References to research not supported by this grant

1) SUBBARAO, E. R. 1987 An experimental investigation of the effects of Reynolds number and Richardson number on the structure of a co-flowing buoyant jet. PhD thesis, Stanford University Department of Aeronautics and Astronautics and SUDAAR 563.

2) MAHALINGAM, S. 1989 Non-premixed combustion: full numerical simulation of a coflowing axisymmetric jet, inviscid and viscous stability analysis. PhD thesis, Stanford University Department of Mechanical Engineering.

References to research supported by AFOSR Grant Number 84-0373 are given in the list of publications on page 12.

PERSONNEL

Dr. C. T. Bowman, Professor

Dr. B. J. Cantwell, Professor

Dr. G. Lewis, Research Assistant - PhD thesis awarded December 1989, thesis title: An experimental investigation of low-speed non-premixed flames and buoyant jets using particle tracking.

Dr. A. Strawa, Research Assistant - PhD thesis awarded June 1986, thesis title: An experimental investigation of the structure of an acoustically excited diffusion flame.

Dr. U. Vandsburger, Research Associate

PUBLICATIONS

1) STRAWA, A W., and CANTWELL, B. J., 1985 Visualization of the structure of a pulsed methane-air diffusion flame. *The Physics of Fluids* **28**, pp. 2317-2320.

2) STRAWA, A. W. and B. J. CANTWELL, 1985 The effect of pressure variation on the structure of a pulsed methane-air diffusion flame. Paper WSS/CI 85-25 presented at the Western States Section of the Combustion Institute Fall Meeting, U.C. Davis, October.

3) STRAWA, A. W., 1986 An experimental investigation of the structure of an acoustically excited diffusion flame. Stanford University Department of Aeronautics and Astronautics Ph.D. thesis and SUDAAR 558, August.

4) VANDSBURGER, U., LEWIS, G., SEITZMAN,J. M., ALLEN,M. G., BOWMAN, C. T.and HANSON, R. K. 1986 Flame-flow structure in an acoustically driven jet flame. Paper 86-19, presented at the Western States Combustion Institute Meeting.

5) LEWIS, G.S., CANTWELL, B.J. and LECUONA, A. 1987 The use of particle tracking to obtain planar velocity measurements in an unsteady laminar diffusion flame." Paper 87-35, presented at the Western States Combustion Institute Meeting, Provo, Utah, April 6-7.

6) STRAWA, A. W. and CANTWELL, B. J. Investigation of an excited jet diffusion flame at elevated pressure. *Journal of Fluid Mechanics* Vol **200**, pp.309-336.

7) LEWIS, G. S., CANTWELL, B. J., VANDSBURGER, U. and BOWMAN, C. T. 1988 An investigation of the structure of a laminar, non-premixed flame in an unsteady vortical flow. Twenty-Second Symposium (International) on Combustion / The Combustion Institute, pp. 515-522.

8) CHONG, M. S., PERRY, A. E. and CANTWELL, B. J. 1989 A general classification of three-dimensional flow patterns. *The Physics of Fluids* (to appear) and SUDAAR 572.

9) CANTWELL, B. J., LEWIS, G. S., and CHEN, J. 1989 Topology of variable density flows. Keynote paper to be presented at the 10th Australasian Fluid Mechanics Conference, December, Melbourne, Australia.

10) LEWIS, G. S. 1989 An experimental investigation of low-speed non-premixed flames and buoyant jets using particle tracking. PhD. thesis, Department of Mechanical Engineering, Stanford University.

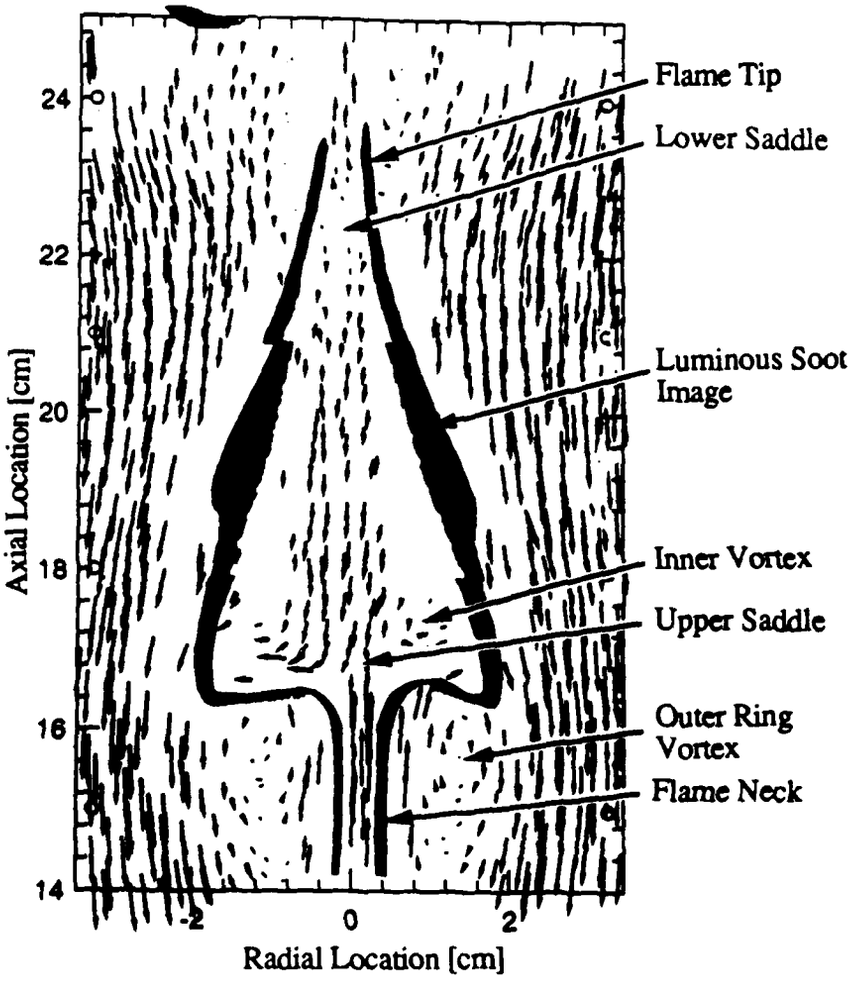

Figure 1 - A typical velocity vector field for the flame showing several key elements of the flame and flow field.

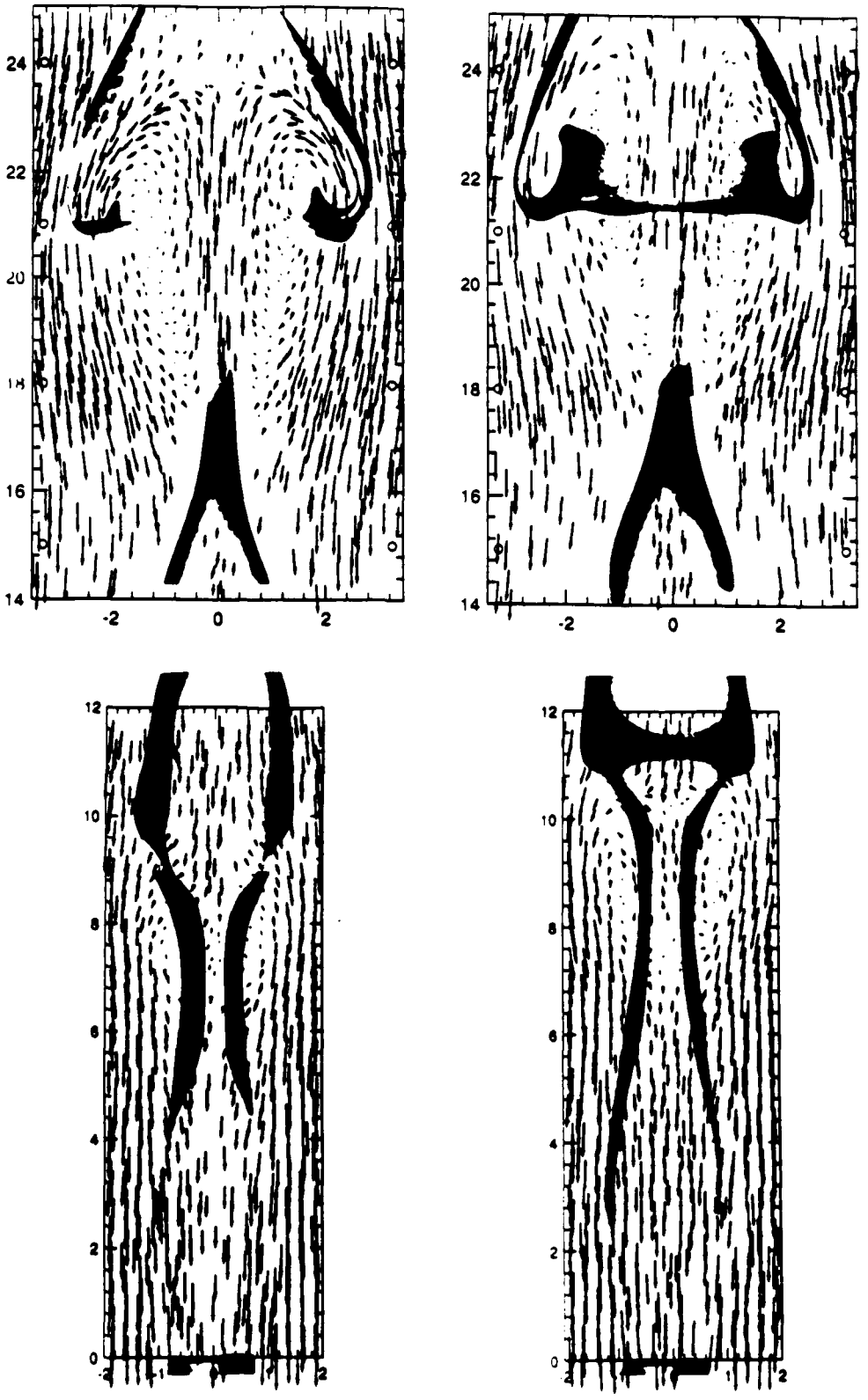

Figure 2 a - A series of eight velocity vector field plots for the measured flame data. The reversed luminous flame image is superimposed for reference.

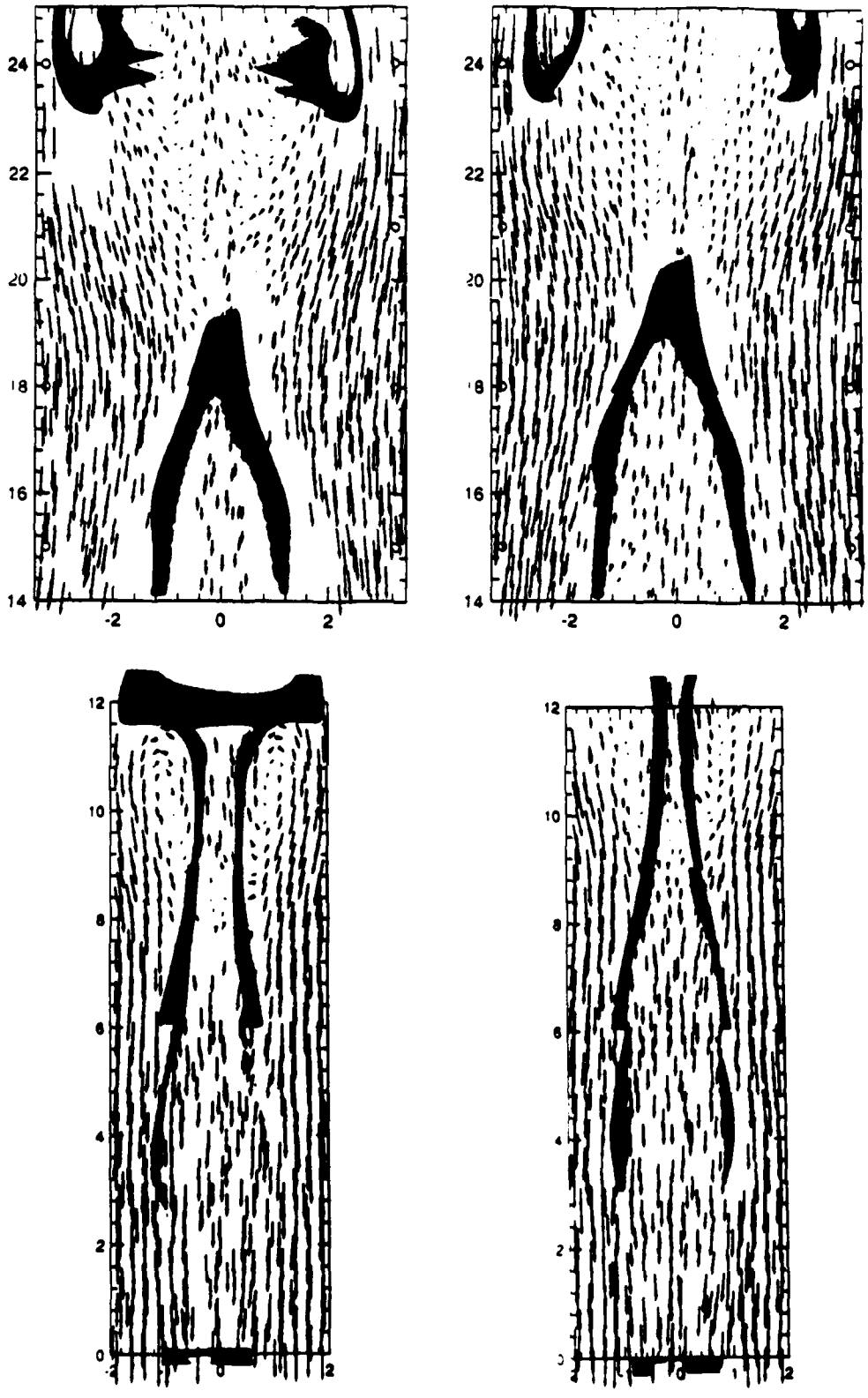

Figure 2 b

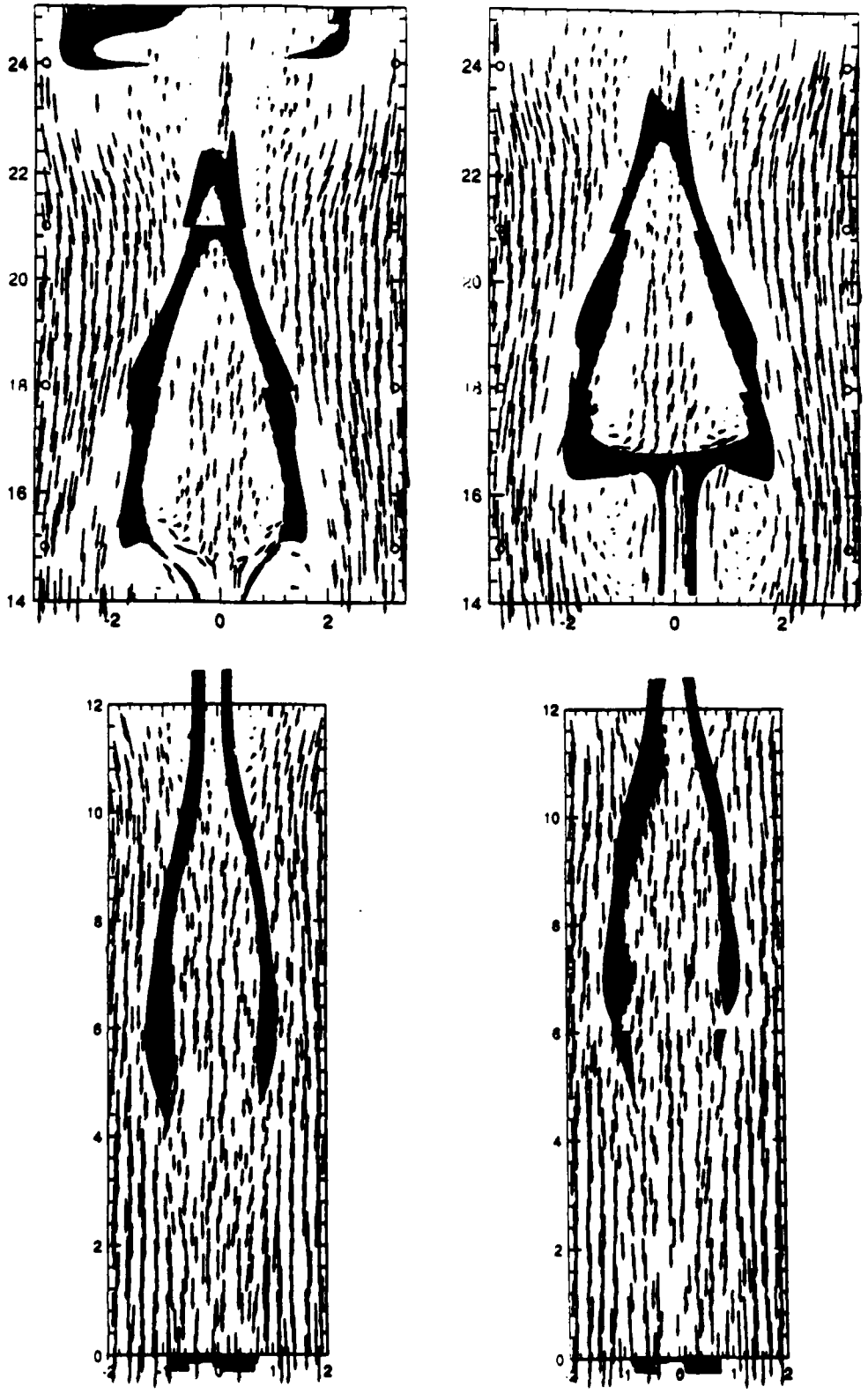

Figure 2 c

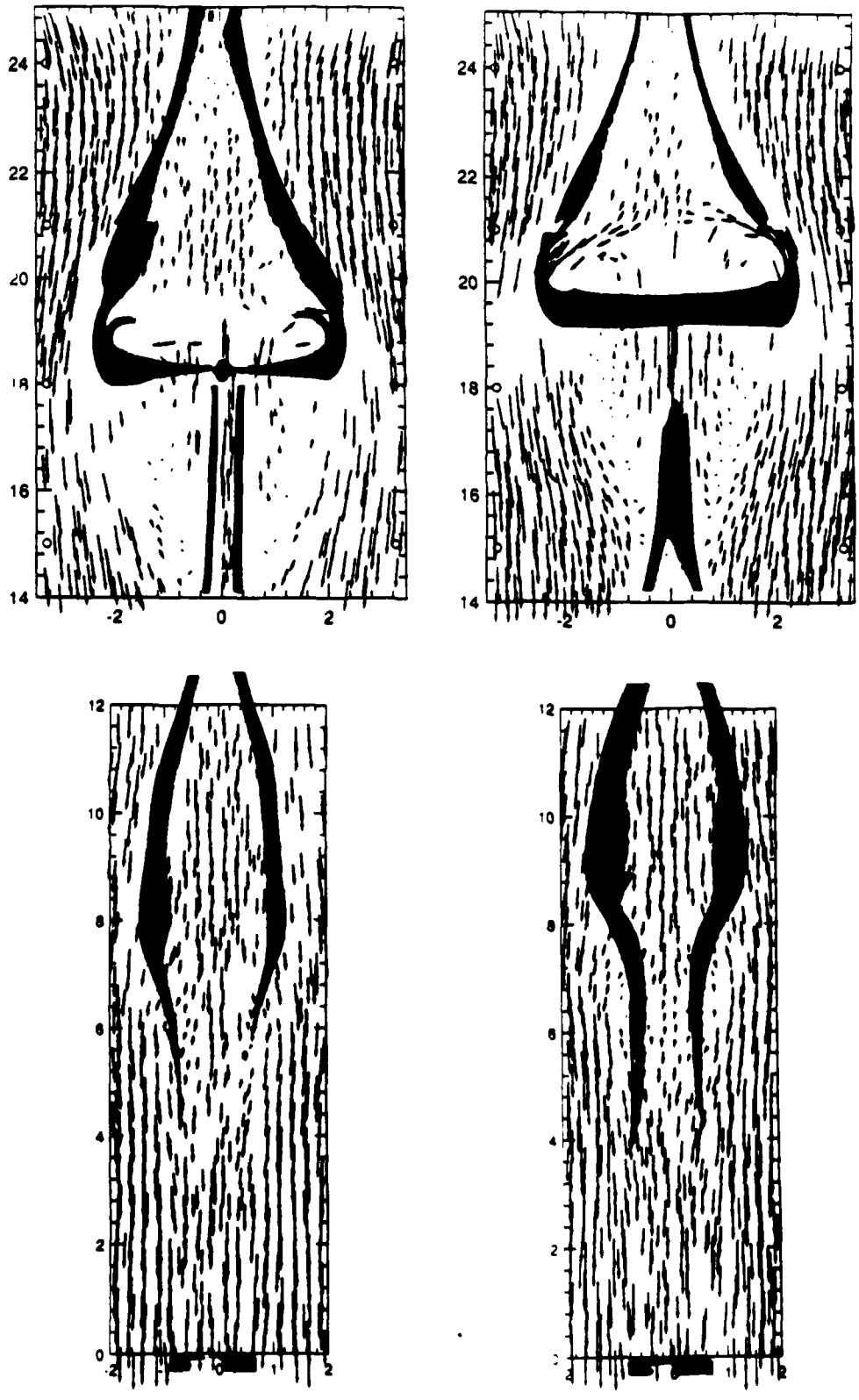

Figure 2 d

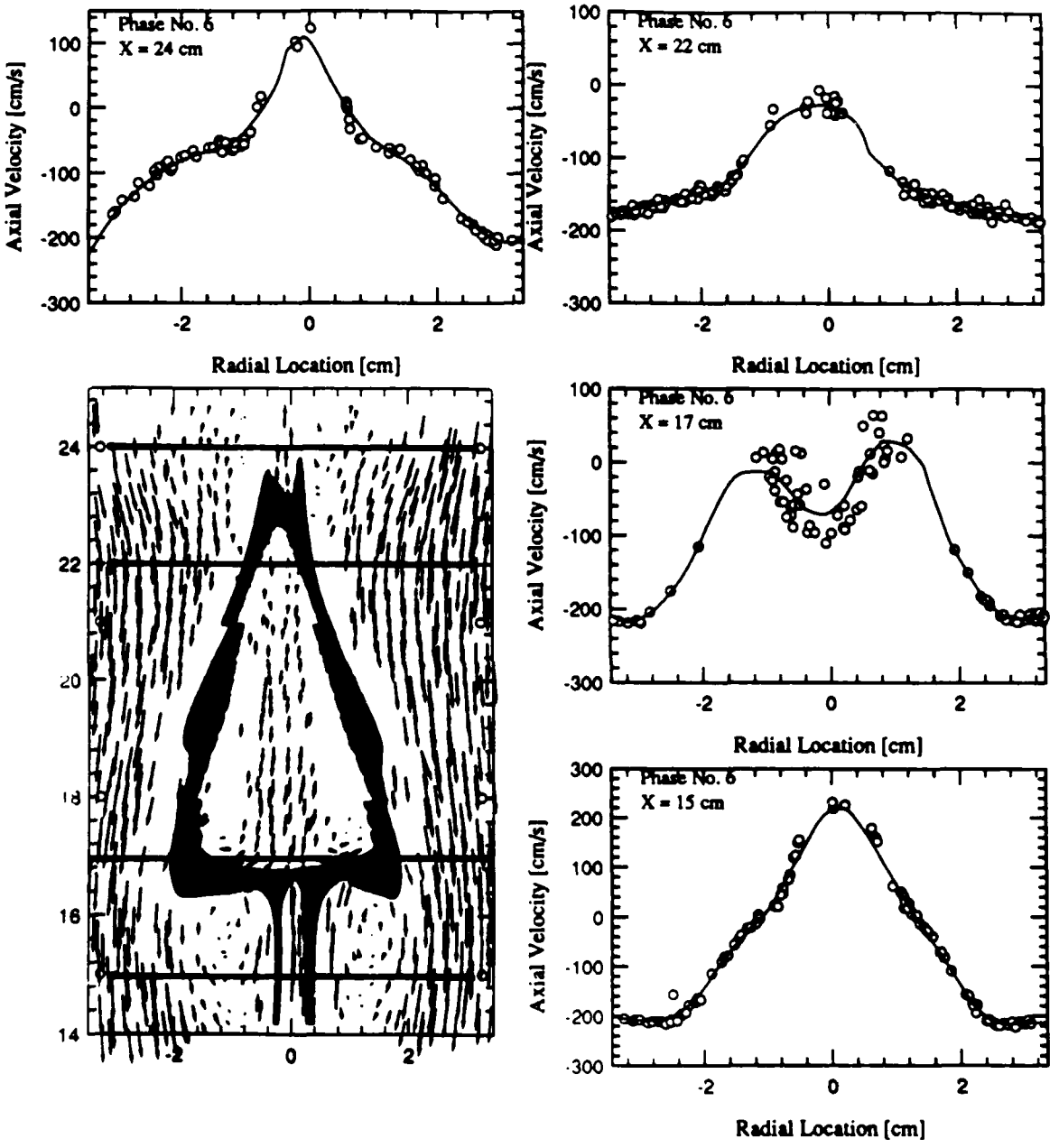

Figure 3 a - Representative axial velocity profiles taken from the velocity data of phase six. The solid line is the interpolation function.

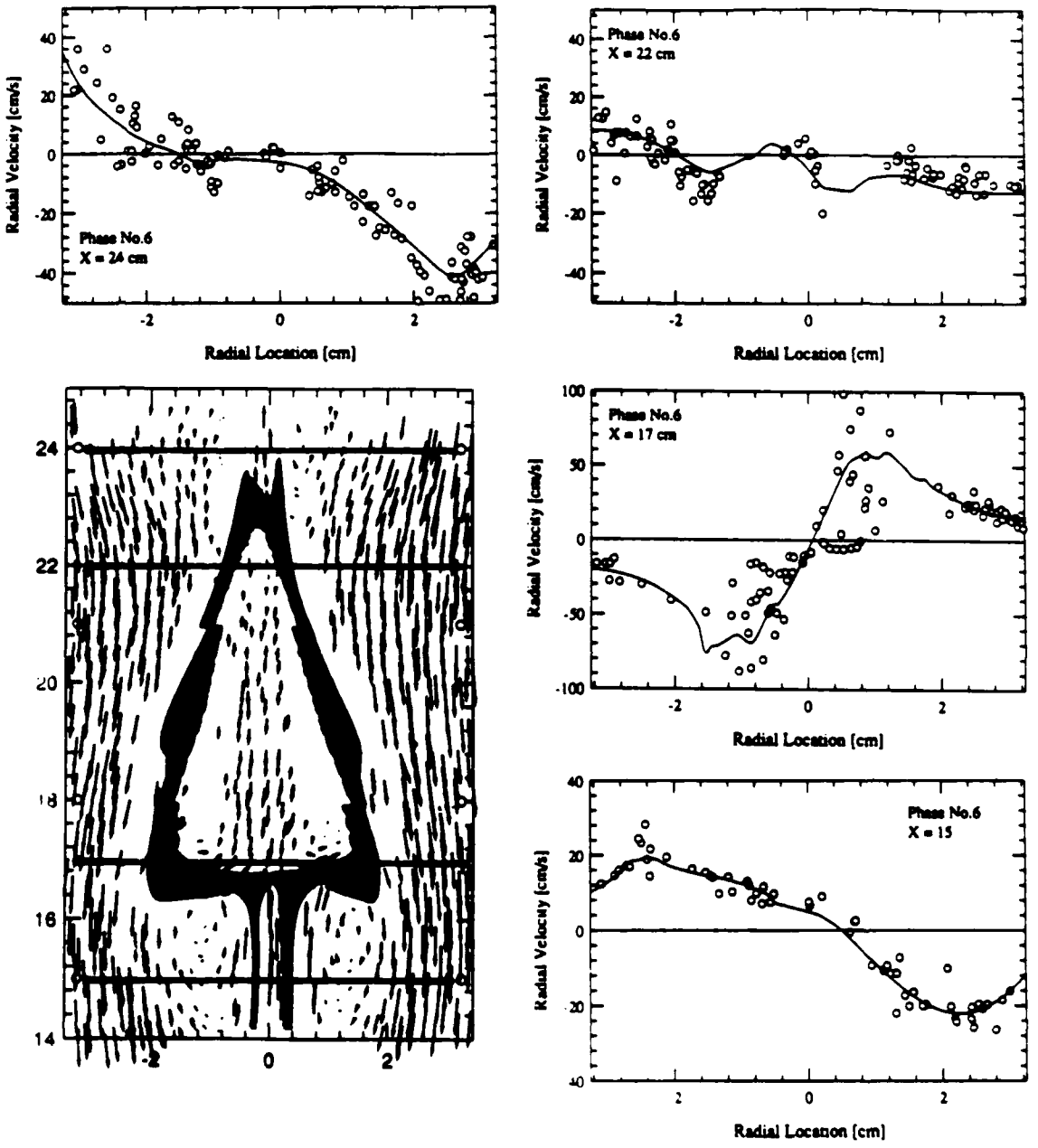

Figure 3 b - Representative radial velocity profiles taken from the velocity data of phase six. The solid line is the interpolation function.

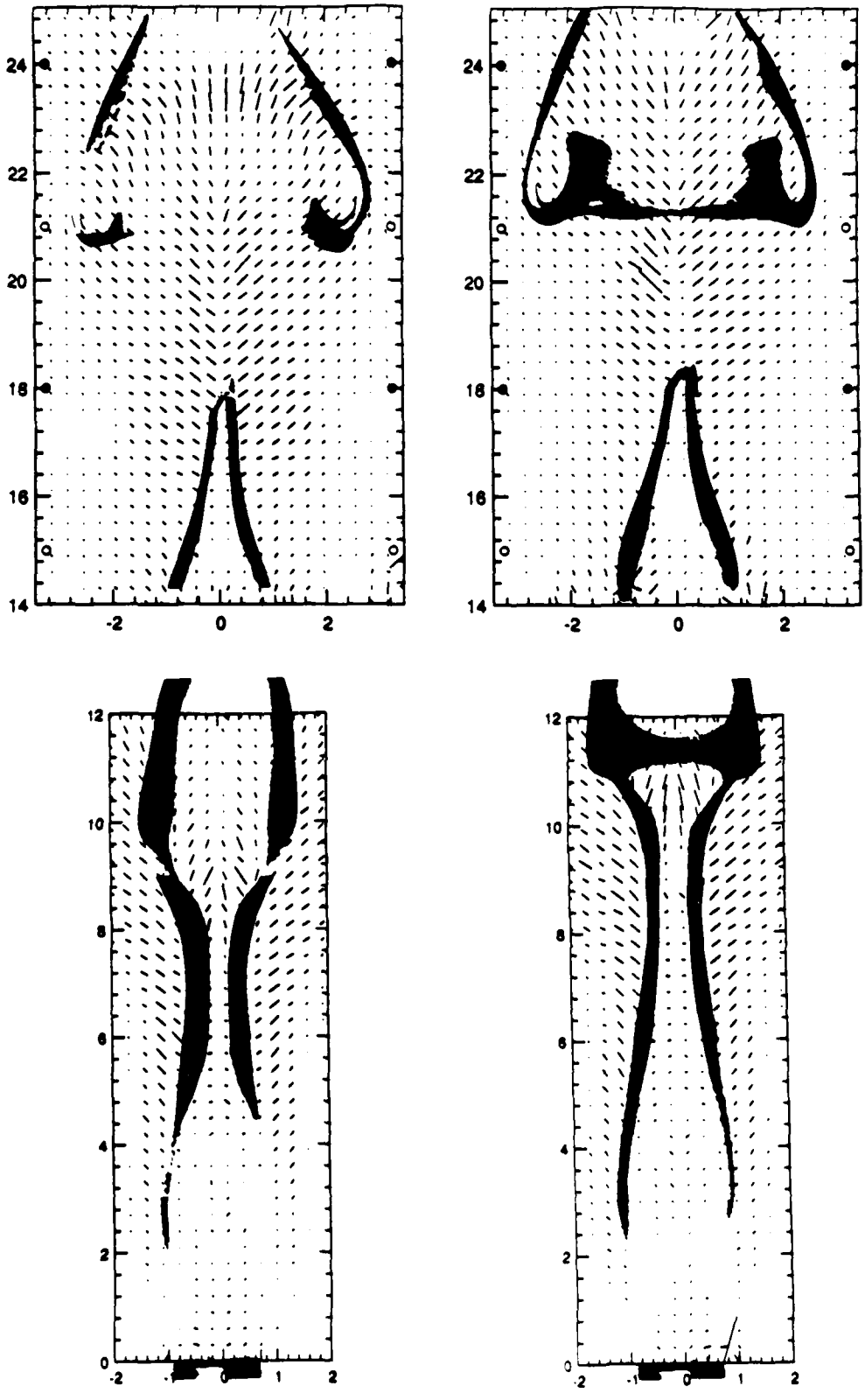

Figure 4 a - A series of eight vector plots showing the direction and magnitude of principal compressive strain rate in the flame.

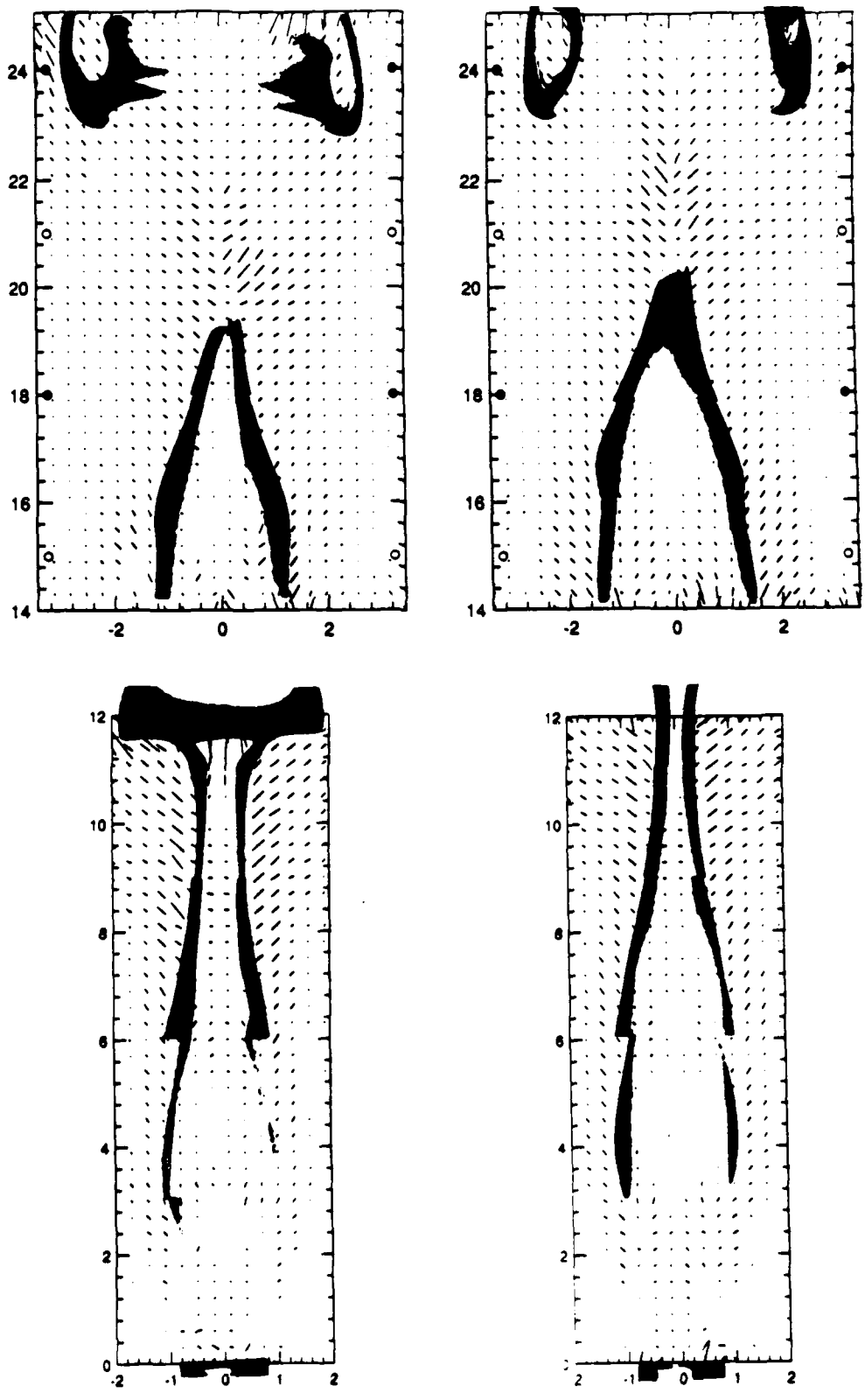

Figure 4 b

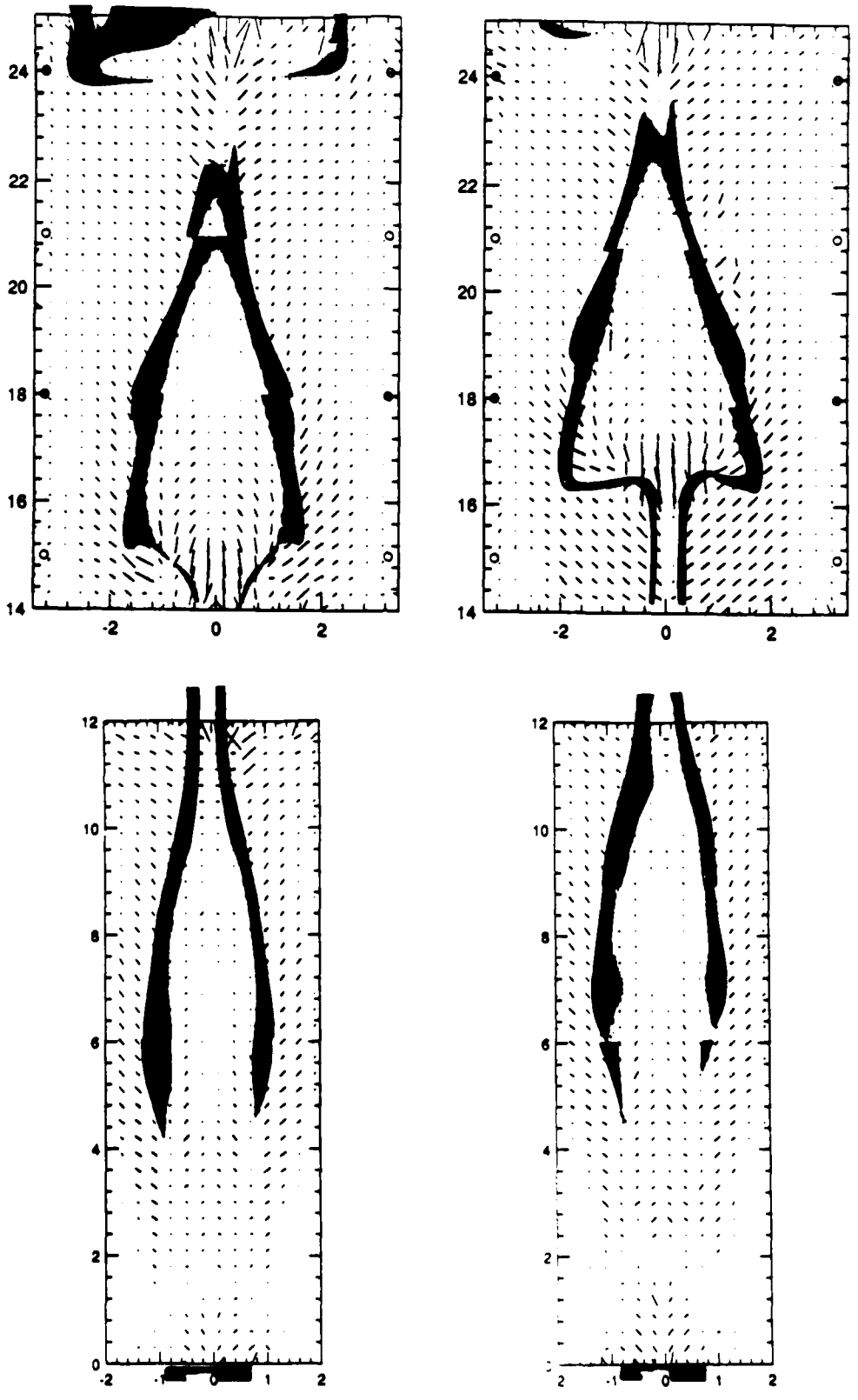

Figure 4 c

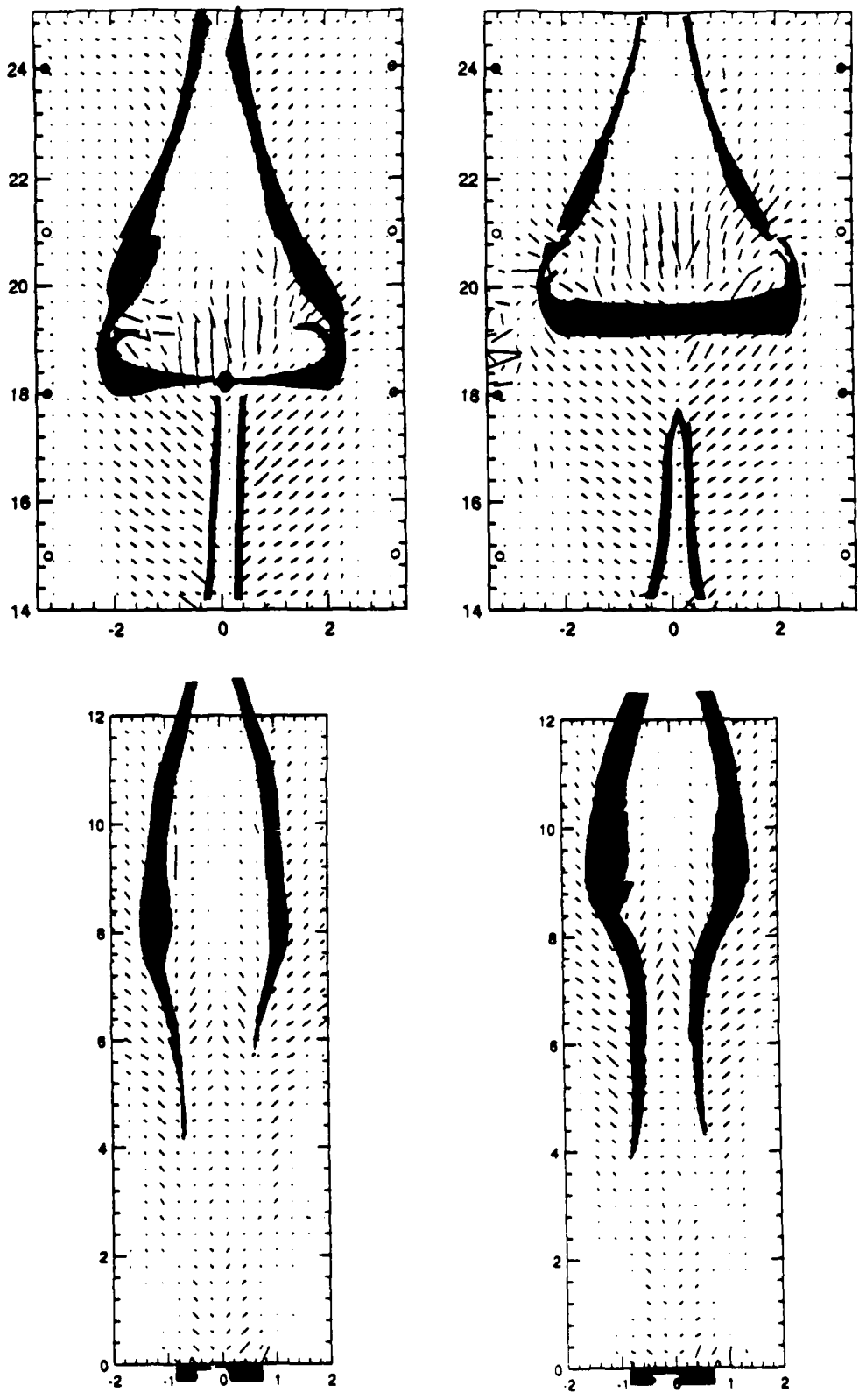

Figure 4 d

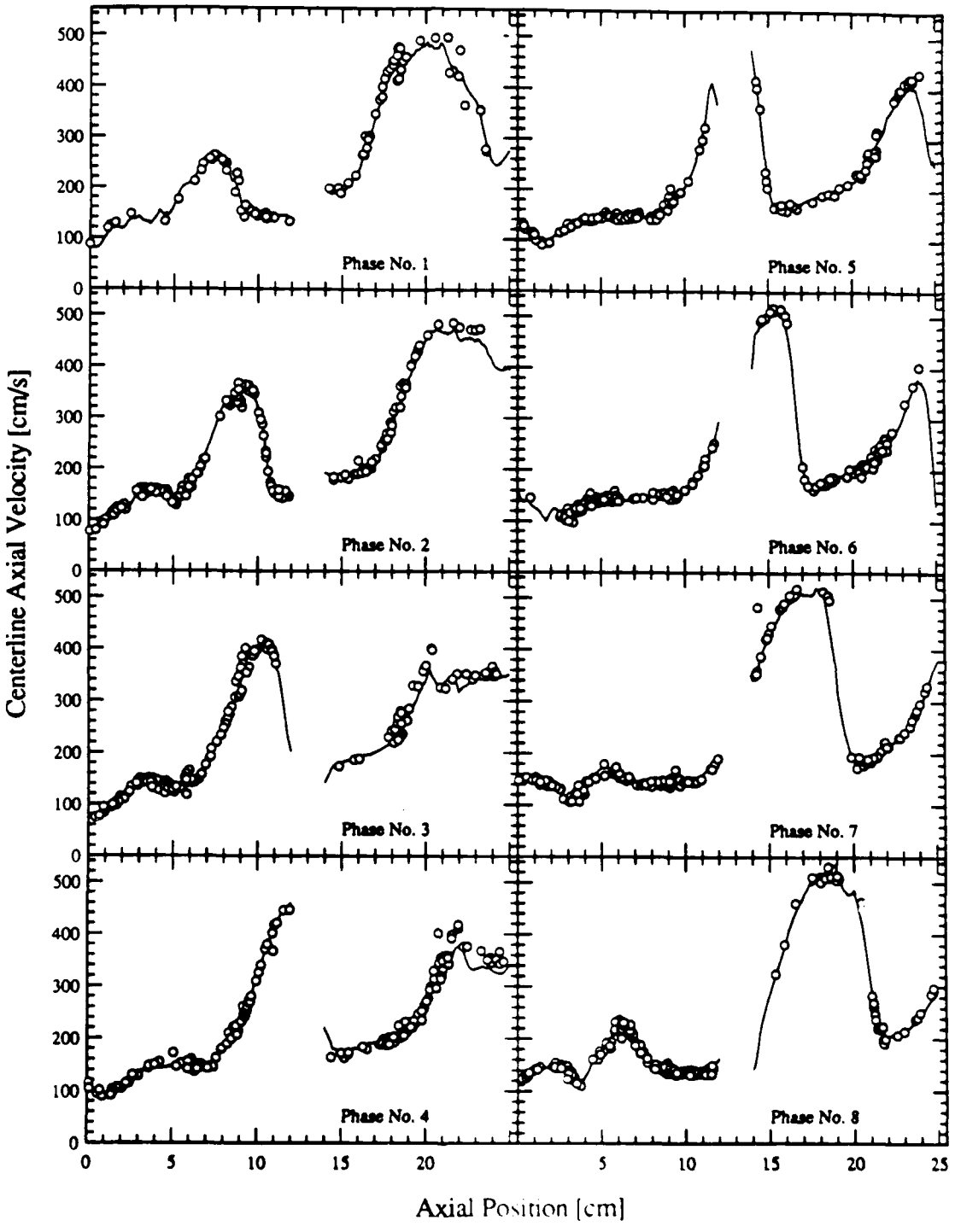

Figure 5 - Centerline axial velocity distributions in the flame at various phases.

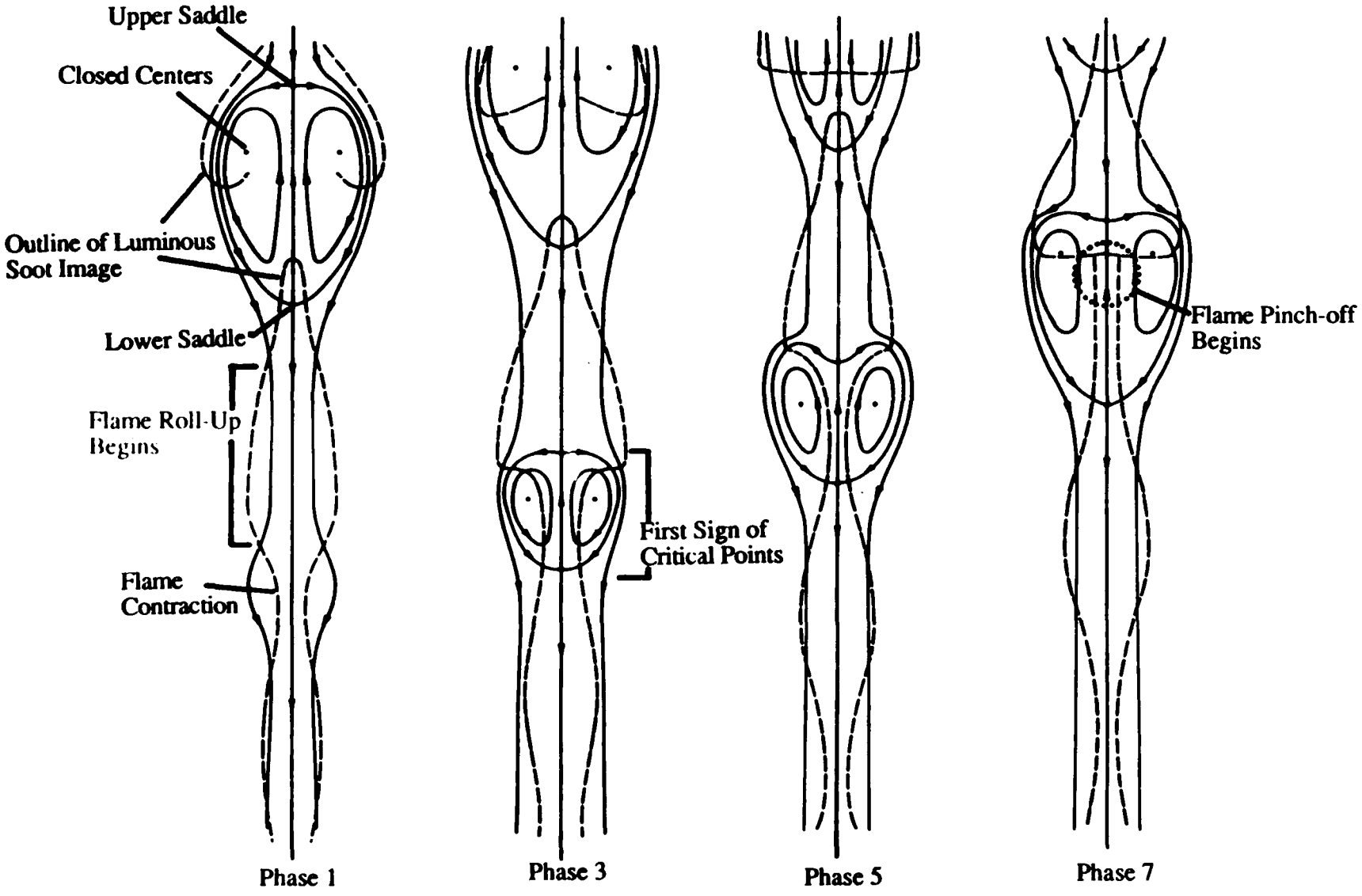

Figure 6 - Sequence of frames showing flame pinch-off.

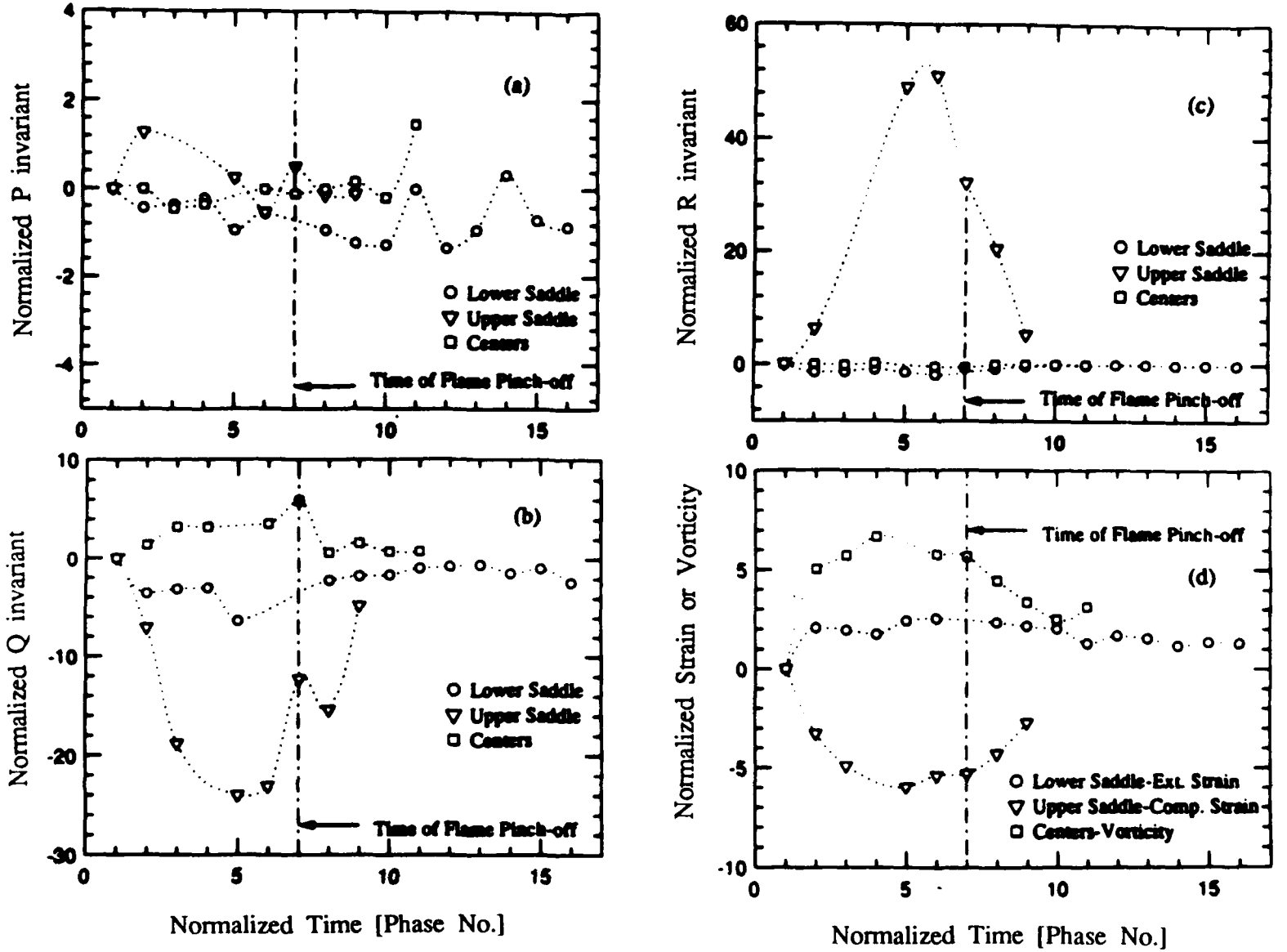

Figure 7 - Evolution of the invariants of the deformation tensor evaluated at the critical points in the flame; (a) the trace, P, (b) the sum of cofactors Q, (c) the determinant, R, and (d) strain and vorticity.

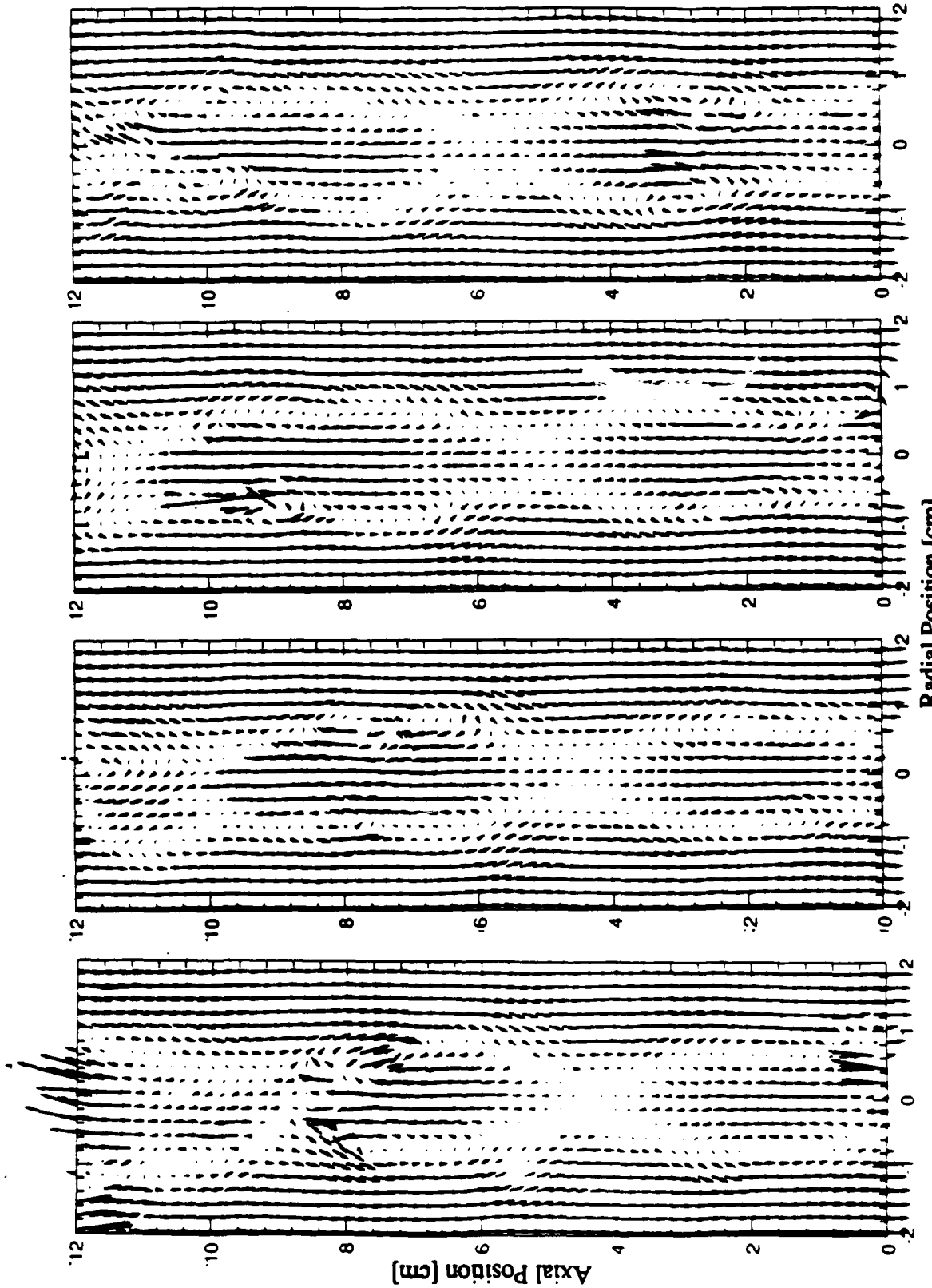

Figure 8 a - A series of eight velocity vector field plots for the interpolated helium data.

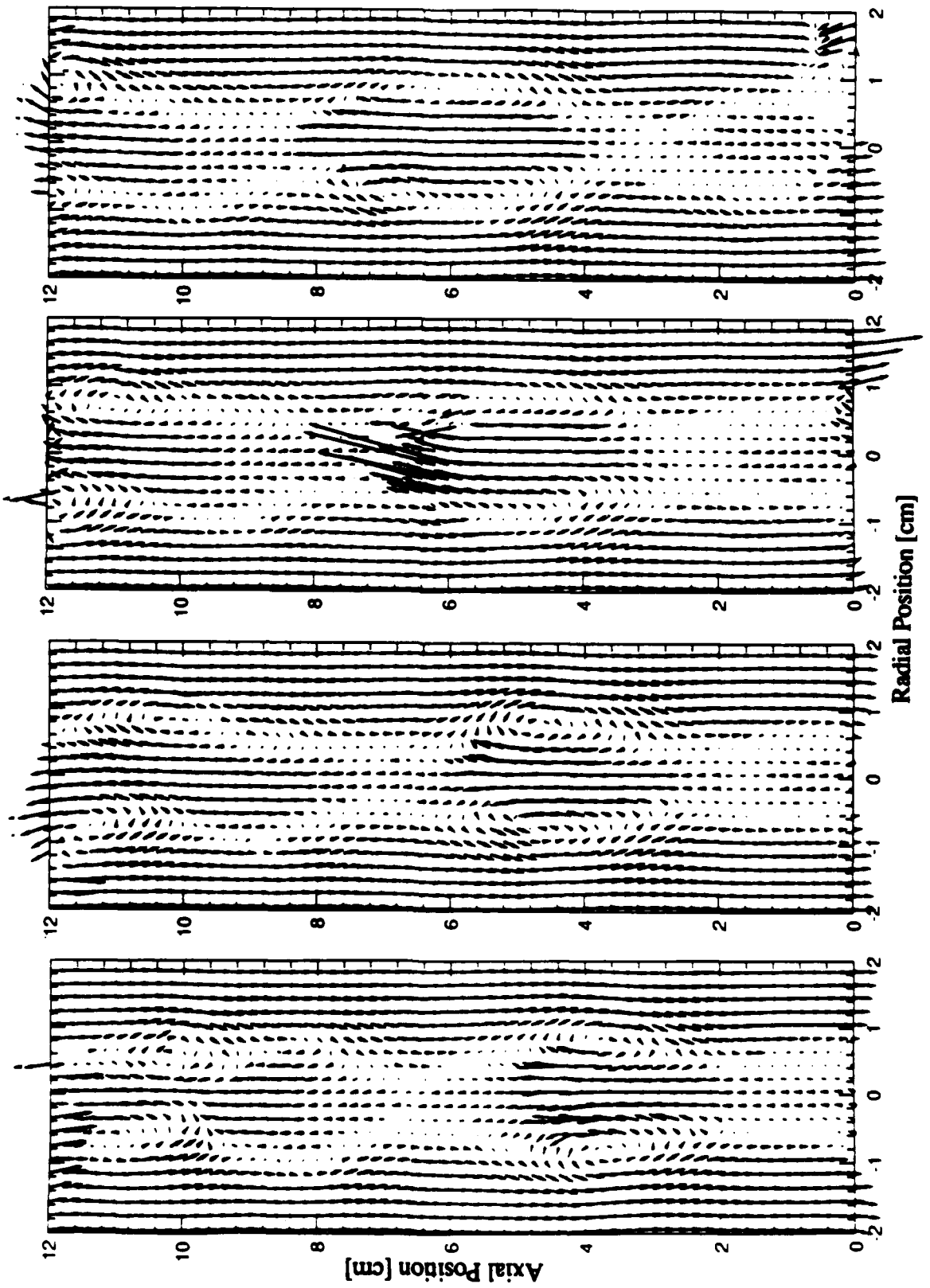

Figure 8 b

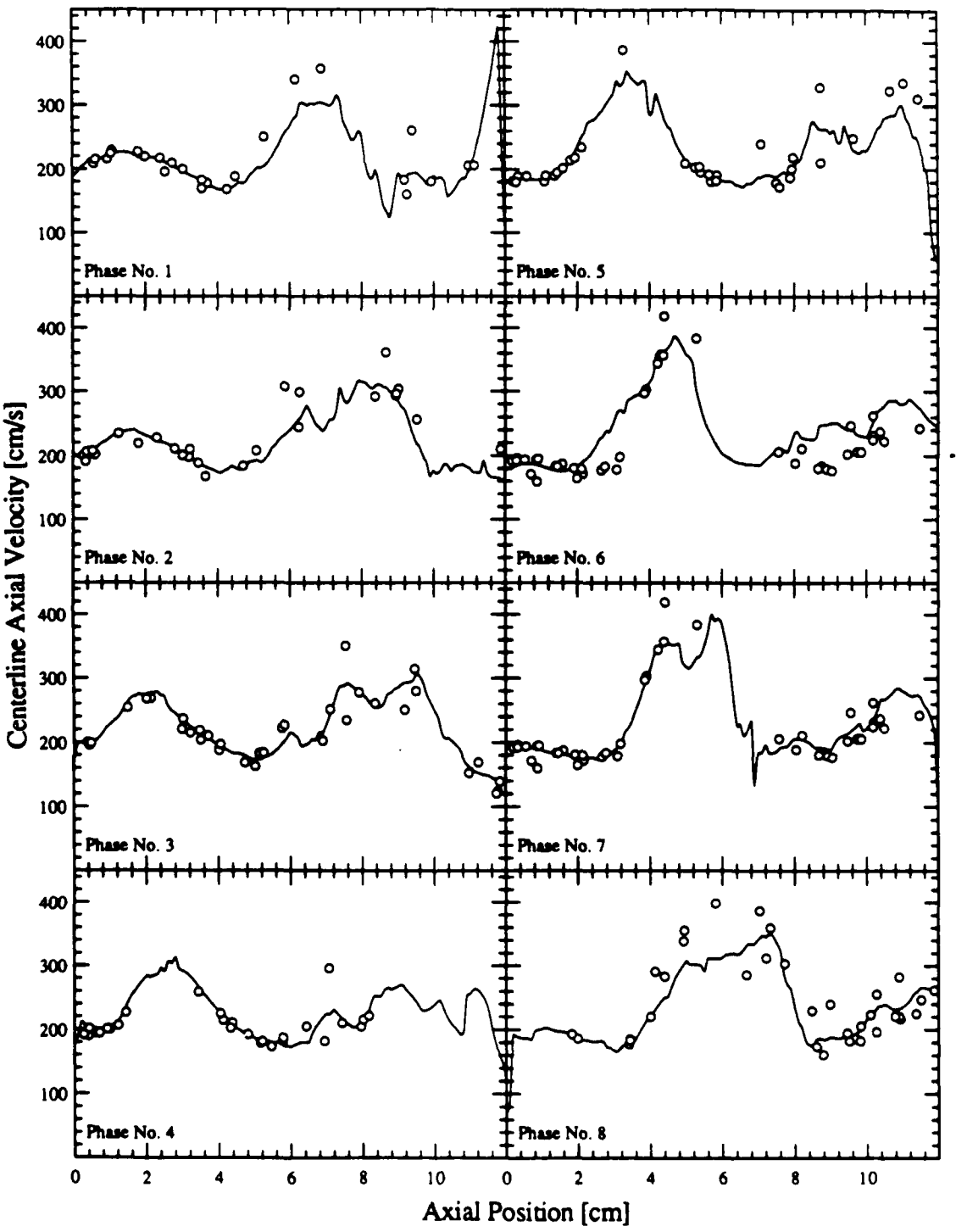

Figure 9 - Centerline axial velocity distributions in the helium jet at various phases.

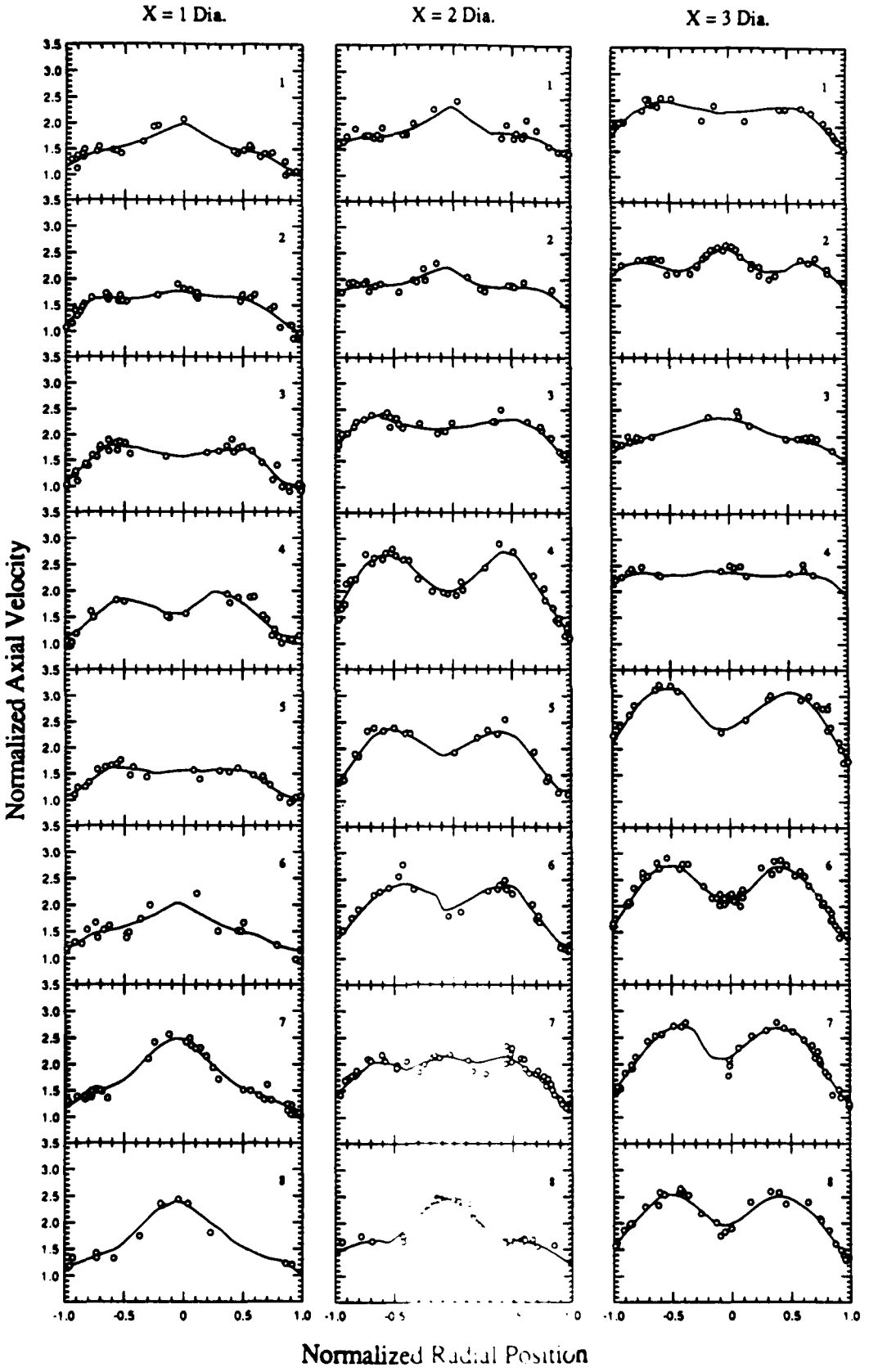

Figure 10 - Normalized axial velocity plots for three streamwise locations in the near field of the flame for all phase locations.

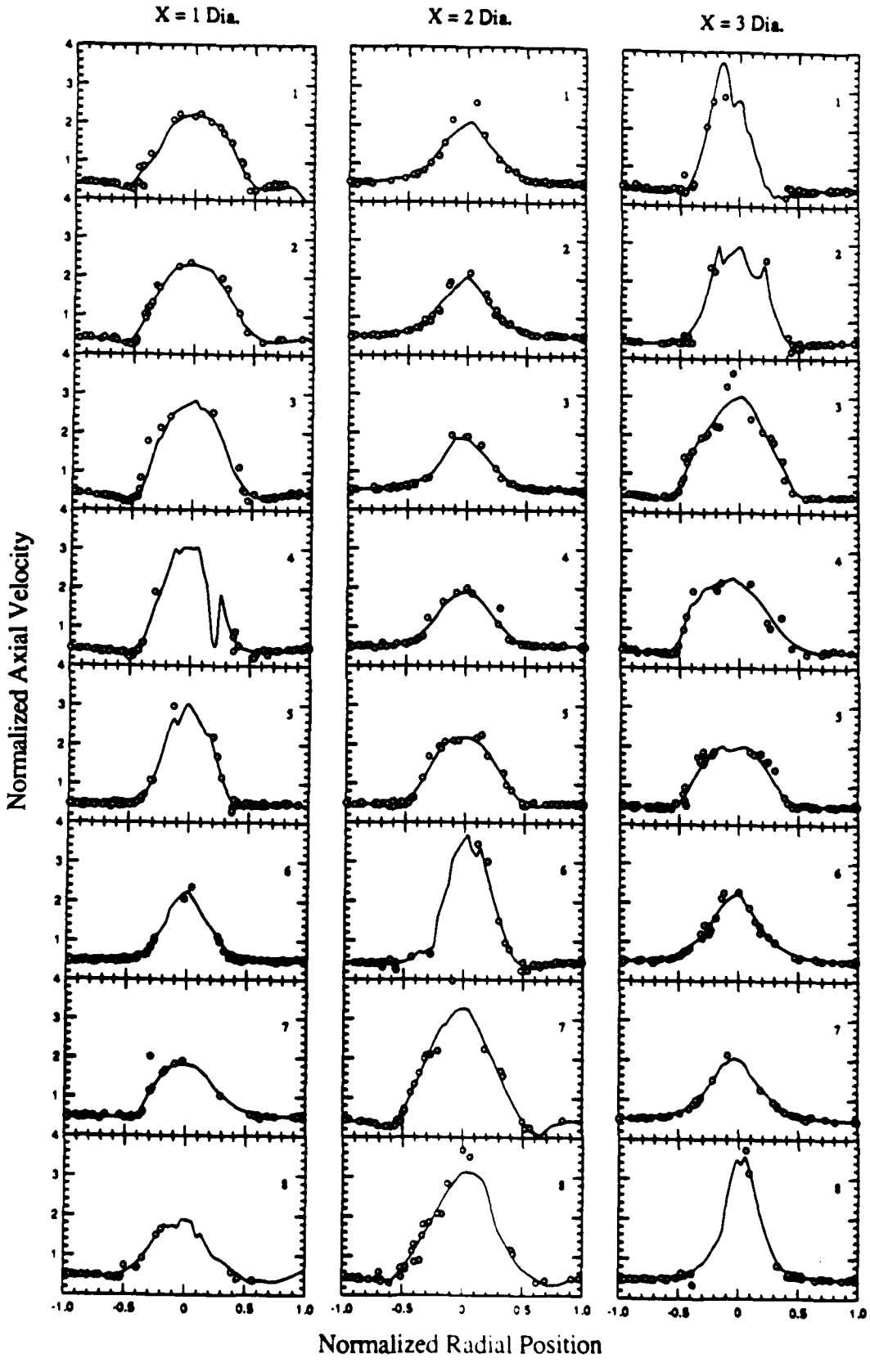

Figure 11 - Normalized axial velocity plots for three streamwise locations in the near field of the helium jet for all phase locations.